

## Scaling in dimer breaking by impurities in $\text{CuGeO}_3$ : A comparative experimental study of Zn-, Mg-, Ni-, and Si-doped single crystals

B. Grenier,\* J.-P. Renard, and P. Veillet

*Institut d'Electronique Fondamentale, Université Paris-Sud, Bâtiment 220, 91405 Orsay Cedex, France*

C. Paulsen

*Centre de Recherche sur les Très Basses Températures, CNRS BP166, 38042 Grenoble Cedex 9, France*

G. Dhalenne and A. Revcolevschi

*Laboratoire de Chimie des Solides, Université Paris-Sud, Bâtiment 414, 91405 Orsay Cedex, France*

(Received 30 June 1998)

We have performed magnetic susceptibility measurements on single crystals of the doped spin-Peierls system  $\text{Cu}_{1-x}M_x\text{GeO}_3$  with  $M = \text{Zn, Mg, Ni}$  ( $0 \leq x \leq 0.06$ ) and made a comparison with our previous results obtained in  $\text{CuGe}_{1-y}\text{Si}_y\text{O}_3$  single crystals. All these substitutions were found to have three major effects: the drastic destruction of the spin-Peierls phase, the appearance at low temperature of a three-dimensional antiferromagnetic order, and the freeing of some  $S = 1/2$  spins. Moreover, doped  $\text{CuGeO}_3$  shows a universal character for the  $[T, x(y)]$  phase diagram and for the doping level dependence of the proportions of free and dimerized spins, with a scaling factor  $x \approx 3y$ . Ni-doping induces a Cu-Ni antiferromagnetic interaction and changes the easy axis in the antiferromagnetic phase. [S0163-1829(98)05738-5]

The discovery of a spin-Peierls (SP) phase in the inorganic compound  $\text{CuGeO}_3$  (Ref. 1) has strongly renewed interest in the SP transition. The  $S = 1/2$   $\text{Cu}^{2+}$  Heisenberg antiferromagnetic (AF) chains become dimerized below spin-Peierls temperature  $T_{\text{SP}} = 14.25$  K, leading to the formation of a singlet ground state separated from the first excited states by an energy gap  $\Delta \approx 23$  K. The SP transition is evidenced by a kink at  $T_{\text{SP}}$  in the magnetic susceptibility and is clearly revealed by x-ray and elastic neutron scattering.<sup>2</sup> The effect of doping has been studied by many authors: Si-substitution for Ge,<sup>3</sup> and Zn, Mg, Ni-substitution for Cu (Ref. 4) induce a strong decrease of  $T_{\text{SP}}$  and the occurrence of a three-dimensional (3D) AF order at lower temperature. However, because the samples used in these studies were not always single crystals and were not systematically analyzed, the temperature-concentration phase diagrams  $(T, x)$  found in the literature are quantitatively different from one author to another and from a type of dopant to another.

The aim of this paper is to make a careful comparative study of  $\text{Cu}_{1-x}M_x\text{GeO}_3$  (with  $M = \text{Zn, Mg, Ni}$ ) and  $\text{CuGe}_{1-y}\text{Si}_y\text{O}_3$  compounds. All of our measurements were performed on high quality single crystals that were analyzed in order to know the effective doping level. We have made extensive magnetic susceptibility measurements on these samples. The  $[T, x(y)]$  phase diagrams are presented and a detailed analysis of the low temperature ( $T < T_{\text{SP}}$ ) susceptibility data is reported, followed by a study of the data obtained for the paramagnetic phase.

The  $\text{Cu}_{1-x}M_x\text{GeO}_3$  single crystals were grown from the melt using a floating zone method associated with an image furnace<sup>5,6</sup> and were analyzed using inductively coupled plasma atomic emission spectroscopy (ICP/AES). The doping levels that will be reported are thus the effective ones derived from the ICP/AES analysis which are usually

slightly lower than the nominal concentration. The magnetic susceptibility was measured using two SQUID magnetometers, one operating in the temperature range 1.8–350 K, the other operating at very low temperature, down to 0.05 K.<sup>7</sup> The temperature dependence of the static susceptibility  $[\chi(T) = M(T)/H]$  was measured for all our Zn, Mg, and Ni-doped samples up to 300 K in a 1 kOe magnetic field applied along the  $c$ -axis (chain direction). For the Ni-doped samples,  $\chi$  was also measured along the  $a$  and  $b$ -axis.

*Low temperature part of the susceptibility.* Figure 1 shows the data obtained below 16 K in 0.8% Ni and 0.7% Zn-doped  $\text{CuGeO}_3$ . The decrease of  $T_{\text{SP}}$  upon doping and the occurrence at low temperature of a 3D-AF order are clearly seen. In Ni-doped  $\text{CuGeO}_3$ , the easy axis is mainly along the

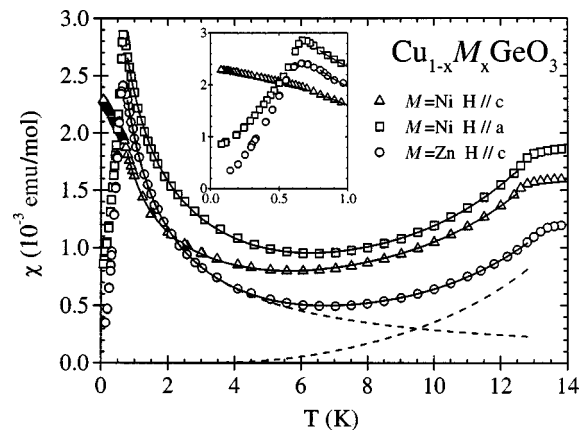


FIG. 1. Temperature dependence of the molar susceptibility measured in 0.8% Ni and in 0.7% Zn-doped  $\text{CuGeO}_3$  (open symbols), and fit between  $T_N$  and  $T_{\text{SP}}$  of each  $\chi(T)$  curve to Eq. (1) (solid lines). The two contributions of Eq. (1),  $\chi_0(x) + K_{\text{PARA}}(x)C/(T - \Theta)$  and  $K_{\text{SP}}(x)\chi_{\text{SP}}(T)$ , are also plotted for the Zn-doped sample (dashed lines).

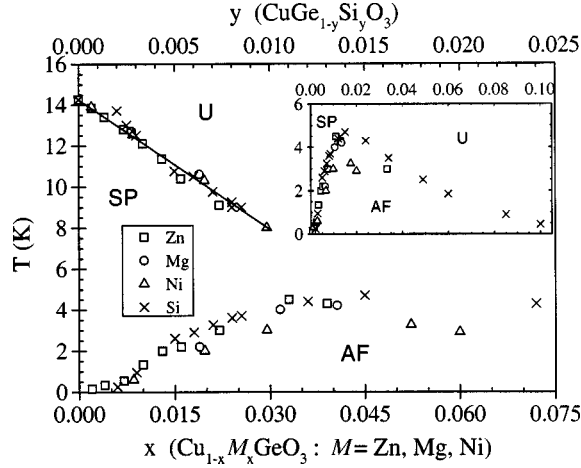


FIG. 2.  $[T, x(y)]$  phase diagram of  $\text{Cu}_{1-x}M_x\text{GeO}_3$  with  $M = \text{Zn}, \text{Mg}, \text{Ni}$ , and  $\text{CuGe}_{1-y}\text{Si}_y\text{O}_3$ , using the scaling  $y = 3x$ . Within this scaling, one can notice the universal character of the phase diagram, except for the  $T_N(x)$  data in Ni-doped  $\text{CuGeO}_3$ . The solid line is described by the equation  $T_{\text{SP}}(x) = T_{\text{SP}}(0)[1 - 15x]$ .

$a$ -axis<sup>8</sup> unlike Zn and Mg-doped  $\text{CuGeO}_3$  where it is along the  $c$ -axis.  $T_{\text{SP}}$  and the Néel temperature ( $T_N$ ) were determined in all our samples, and are defined as temperatures giving the maximum of  $d\chi/dT$  and  $d(\chi T)/dT$  respectively (see Ref. 7). The resulting  $(T, x)$  phase diagram is presented in Fig. 2. One can notice that the  $\text{Cu}_{1-x}M_x\text{GeO}_3$  compounds display the same phase diagram for  $M = \text{Zn}, \text{Mg}$ , and  $\text{Ni}$ , although the  $T_N(x)$  curve for  $\text{Cu}_{1-x}\text{Ni}_x\text{GeO}_3$  has a maximum at a slightly lower temperature. For these three substitutions, the SP transition line can be well described by the linear equation  $T_{\text{SP}}(x)/T_{\text{SP}}(0) = 1 - \alpha x$  with  $\alpha \approx 15$  (see solid line in Fig. 2), so that  $T_{\text{SP}}(x)$  tends to zero for  $x \approx 0.067$ . In  $\text{CuGe}_{1-y}\text{Si}_y\text{O}_3$ ,  $T_{\text{SP}}(y)$  was found to follow the same simple equation with  $\alpha \approx 44$ .<sup>7</sup> This leads to the scaling  $y \approx 3x$ . The  $T_{\text{SP}}(y)$  and  $T_N(y)$  data from Ref. 7 are also plotted in Fig. 2 using this scaling. Then, the Néel temperatures,  $T_N(x)$  for Zn and Mg, and  $T_N(y)$  for Si, are also coincident. The  $T_N(x)$  data of Zn-doped  $\text{CuGeO}_3$  at low  $x$  suggest the absence of a threshold concentration for the occurrence of the AF phase: The Néel temperature seems to tend to zero as  $x$  tends to zero. Note that it was not possible to make this assumption for  $\text{CuGe}_{1-y}\text{Si}_y\text{O}_3$  (Ref. 7) due to the three times stronger effect of Si-substitution.

For the low concentration ( $x \leq 0.02$ ) Zn, Mg, and Ni-doped samples, we assume that below  $T_{\text{SP}}(x)$  the Cu spins give rise to two main contributions: spin-Peierls (dimerized spins) and paramagnetic (free spins). We thus fit the molar susceptibility data  $\chi(x, T)$  between  $T_N(x)$  and  $T_{\text{SP}}(x)$  to the following relation:

$$\chi(x, T) = \chi_0(x) + K_{\text{PARA}}(x) \frac{C}{T - \theta} + K_{\text{SP}}(x) \chi_{\text{SP}}(T). \quad (1)$$

The first term  $\chi_0$  is a small constant which includes the diamagnetic contributions of both the sample holder and the sample itself as well as the Van Vleck contribution of the sample. The second term represents the paramagnetic Curie-Weiss contribution of a small proportion  $K_{\text{PARA}}(x)$  of  $S = 1/2$  free spins, with  $C$  the molar Curie constant of pure

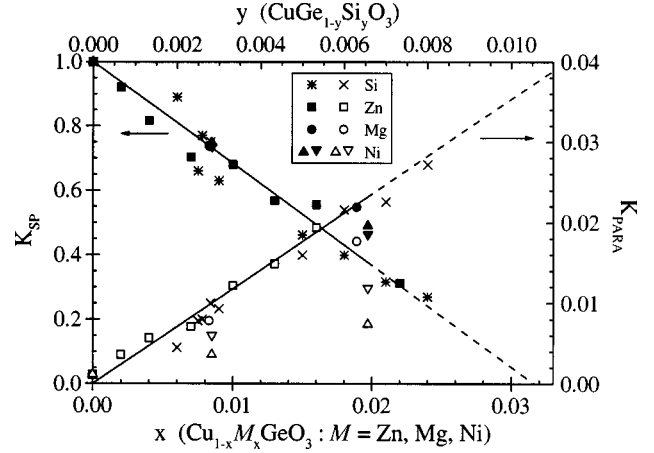


FIG. 3. Doping level dependence of the proportions of spins in the paramagnetic (open symbols) and spin-Peierls (solid symbols) states, for  $\text{Cu}_{1-x}M_x\text{GeO}_3$  and  $\text{CuGe}_{1-y}\text{Si}_y\text{O}_3$ , using the scaling  $y = 3x$ . These two contributions were fitted to a linear law (solid lines) and extrapolated up to  $x \approx 0.03$  ( $y \approx 0.01$ ) (dashed lines). All these data were obtained with  $H \parallel c$ , except the down triangles for which  $H \parallel a$ .

$\text{CuGeO}_3$ . The third term represents the spin-Peierls contribution of a proportion  $K_{\text{SP}}(x)$  of Cu spins which is assumed to have the same temperature dependence, with lower  $T_{\text{SP}}(x)$ , as in the pure sample. Thus we used, for the fits, the phenomenological expression previously established for the pure sample,<sup>7</sup> with no adjustable parameter:

$$\chi_{\text{SP}}(T) = F(t) = (a_0 + a_1 t + a_2 t^2) \exp\left(-\frac{A}{t}\right). \quad (2)$$

In this relation, the exponential function accounts for the presence of the SP gap and  $t$  is the reduced temperature  $T/T_{\text{SP}}(x)$ .

The fits of the  $\chi(T)$  data to expression (1) for  $\text{Cu}_{0.993}\text{Zn}_{0.007}\text{GeO}_3$  (along the  $c$  axis) and for  $\text{Cu}_{0.992}\text{Ni}_{0.008}\text{GeO}_3$  (along the  $c$  and  $a$  axis) are shown in Fig. 1 (solid lines). As expected, the  $\chi_0(x)$  values remain very small and do not depend on the doping level for the Zn and Mg-doped samples ( $|\chi_0| < 0.1 \times 10^{-3}$  emu/mol). However, this is not the case for the Ni-doped samples where  $\chi_0$  increases from 0.45 to  $1.2 \times 10^{-3}$  emu/mol when  $x$  increases from 0.01 to 0.02. This latter observation will be discussed further on. The doping level dependence of the spin proportions  $K_{\text{PARA}}$  and  $K_{\text{SP}}$  is shown in Fig. 3. The  $K_{\text{PARA}}(x)$  and  $K_{\text{SP}}(x)$  data are to a good approximation coincident for the three substitutions, except the values of  $K_{\text{PARA}}(x)$  for Ni, which are on the average two times smaller than for Mg and Zn. These latter values are also slightly different for the  $c$  and  $a$ -axis. The  $K_{\text{PARA}}(x)$  and  $K_{\text{SP}}(x)$  data were fit to the linear laws:

$$K_{\text{PARA}}(x) = ax, \quad (3)$$

$$K_{\text{SP}}(x) = 1 - bx \quad (4)$$

and the following coefficients were obtained:  $a \approx 1.2$  and  $b \approx 32$ . An extrapolation to  $K_{\text{SP}}(x) = 0$  implies that the SP phase would disappear for  $x \approx 0.03$ . The behavior of  $K_{\text{PARA}}(x)$  for Zn or Mg implies that each impurity ion is

responsible for the freeing of about one  $S = 1/2$  spin. Indeed, the substitution of a Cu ion by a nonmagnetic impurity effectively cuts the chain and therefore a dimer, leading to the freeing of one Cu spin. The  $K_{\text{PARA}}(x)$  data for Ni are surprisingly different. Here one would expect the substitution of a Cu ion by a magnetic impurity (Ni:  $S = 1$ ) to lead to the replacement of a dimer by an AF-coupled Cu-Ni pair which should also behave like a free  $1/2$  spin at low temperature (see below). For  $\text{CuGe}_{1-y}\text{Si}_y\text{O}_3$ ,  $K_{\text{PARA}}(y)$  and  $K_{\text{SP}}(y)$  were found to follow Eqs. (3) and (4) with  $a \approx 3.3$  and  $b \approx 98$ ,<sup>7</sup> again leading to the scaling  $y \approx 3x$ . The  $K_{\text{PARA}}(y)$  and  $K_{\text{SP}}(y)$  data from Ref. 7 are also plotted in Fig. 3 using  $y \approx 3x$ .

From this analysis, two points deserve to be discussed.

First, these results show that Si-doping is three times more efficient than  $M$ -doping ( $M = \text{Zn}, \text{Mg}, \text{Ni}$ ) in destroying the SP phase (decrease of  $T_{\text{SP}}$  and of  $K_{\text{SP}}$ ), in restoring an AF phase at low temperature, and in freeing some  $S = 1/2$  spins. This may at first sight seem surprising: Indeed, since Si substitutes between the spin chains while  $M$  substitutes on the spin chains, one could expect Si-doping to be less efficient than  $M$ -doping. However, Khomskii *et al.*<sup>9</sup> have suggested that Si substituted for Ge breaks the superexchange interaction between Cu neighbors on the two Cu chains adjacent to the Si ion. Thus one Si impurity effectively cuts two chains and should therefore be equivalent to two nonmagnetic atoms substituted for Cu, leading to the scaling factor  $y = 2x$ . To explain the observed factor 3, it is necessary to suppose that the two next-neighboring Cu chains are also more or less influenced by Si-doping, but there is no theory about that at this time.

Second, within this ‘‘two contribution model’’ (dimerized and free  $1/2$  spins), one would expect the sum  $K_{\text{PARA}}(x) + K_{\text{SP}}(x)$  to remain equal to 1 for each doping concentration, which is not the case (see Fig. 3). This can be understood if one considers a less naive model where each chain break induces a soliton instead of a simple free  $1/2$  spin. As explained by Khomskii *et al.*,<sup>9</sup> the soliton is located at a distance  $\xi$  ( $\xi \approx 8 - 12$  spins) from impurity, it consists of staggered moments whose amplitude decays over a typical correlation length  $\xi$  and it carries a resulting spin  $S = 1/2$ . Within this region of AF spin correlations, the dimerization is reduced and the phase changes by  $\pi$ . Elsewhere, the dimerization remains unchanged. Note that this approach is rather similar to the model of Fukuyama *et al.*<sup>10</sup> which explains the coexistence of dimerization and antiferromagnetism in  $\text{Cu}_{1-x}\text{Zn}_x\text{GeO}_3$  and  $\text{CuGe}_{1-y}\text{Si}_y\text{O}_3$ . The latter model is supported by muon spin relaxation in Zn and Si-doped  $\text{CuGeO}_3$ .<sup>11,12</sup> If we compare our analysis to the soliton model, the spin-Peierls contribution  $K_{\text{SP}}$  corresponds to the fully dimerized regions (outside the soliton) and the paramagnetic contribution  $K_{\text{PARA}}$  arises from the solitons. However, since about  $2\xi$  spins are involved in each resulting  $S = 1/2$  spin, a physically reasonable approximation is to assume the relation:  $2\xi K_{\text{PARA}}(x) + K_{\text{SP}}(x) \approx 1$  for each doping level. It is in satisfactory agreement with our experimental data of Fig. 3 by using the theoretical value of  $\xi$  cited above.

*High temperature part of the susceptibility ( $T > 20$  K).* Figure 4 shows the temperature dependence of the molar susceptibility measured up to 300 K in pure, 4% Zn, 5% and

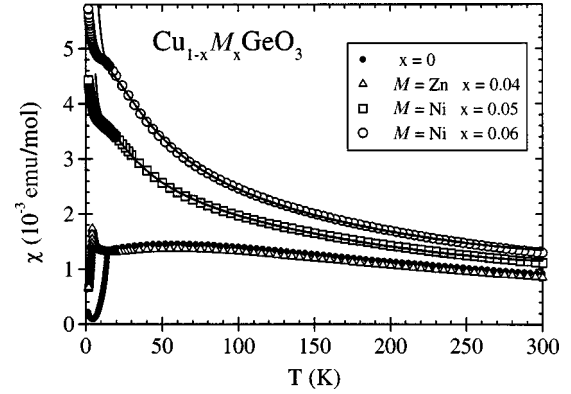


FIG. 4. Temperature dependence of the molar susceptibility measured up to 300 K in a 1 kOe magnetic field applied along the  $c$  direction in pure  $\text{CuGeO}_3$  and in  $\text{Cu}_{1-x}M_x\text{GeO}_3$  with  $M = \text{Zn}, \text{Ni}$ . The solid lines are the fits to Eq. (7).

6% Ni-doped  $\text{CuGeO}_3$ . Between 20 and 300 K, the susceptibility of all our  $\text{Cu}_{1-x}M_x\text{GeO}_3$  samples, with  $M = \text{Zn}$  and  $\text{Mg}$  ( $S = 0$ ),  $\chi_{M,x}$ , can be scaled to the susceptibility of pure  $\text{CuGeO}_3$ ,  $\chi_{\text{pure}}$  by the following relation (see Fig. 4):

$$\chi_{M,x}(T) = (1-x)\chi_{\text{pure}}(T). \quad (5)$$

For  $\text{CuGe}_{1-y}\text{Si}_y\text{O}_3$ , the susceptibility between 20 and 300 K is equal to that of pure  $\text{CuGeO}_3$ . These results signify that the nonmagnetic impurities, substituted either on the Cu or the Ge site, are essentially invisible in the paramagnetic phase: The Cu spins behave exactly like the Cu spins of pure  $\text{CuGeO}_3$  in respective amounts  $1-x$  and 1.

As can be seen in Fig. 4, Ni impurities ( $S = 1$ ) behave in a very different way. The susceptibility increases as temperature decreases, and this trend is stronger for higher Ni-doping values. The kink observed around 10 K in the susceptibility curves suggests the presence of an energy gap. To describe the susceptibility of  $\text{Cu}_{1-x}\text{Ni}_x\text{GeO}_3$  in the paramagnetic phase, a very simple model was chosen. It was assumed that the total susceptibility can be decomposed into two contributions: the susceptibility of a proportion  $(1-2x)$  of pure  $\text{CuGeO}_3$  and that of a proportion  $x$  of Cu-Ni pairs. We consider that  $\text{Cu}^{2+}$  ( $S = 1/2$ ) and  $\text{Ni}^{2+}$  ( $S' = 1$ ) are AF-coupled within one pair (exchange interaction  $J_{\text{Ni-Cu}}$ ), and that these pairs are independent of each other and from the rest of the Cu spins. Then, each Cu-Ni pair can be described by the Hamiltonian  $H = J_{\text{Ni-Cu}}\mathbf{S} \cdot \mathbf{S}'$  and its susceptibility is found to be equal to

$$\chi_{\text{Ni-Cu}}(T) = \frac{1 + 10 \exp(-\Delta/kT) \frac{(g\mu_B)^2}{4kT}}{1 + 2 \exp(-\Delta/kT)}, \quad (6)$$

where  $\Delta = 3/2 J_{\text{Ni-Cu}}$  is the energy gap,  $\mu_B$  the Bohr magneton,  $k$  the Boltzmann constant and we suppose  $g = 2$ . Thus, each Cu-Ni pair is equivalent to a free  $S = 1$  spin and a free  $S = 1/2$  spin at high temperature and to a free  $S = 1/2$  spin at low temperature, which is in agreement with our previous interpretation in the SP phase. For each  $\text{Cu}_{1-x}\text{Ni}_x\text{GeO}_3$  sample, the molar susceptibility (measured along the  $a$ ,  $b$  and  $c$  directions) was fitted between 20 and 300 K to the following expression (see Fig. 4):

$$\chi(T) = \chi_0 + (1 - 2x')\chi_{\text{pure}}(T) + x'N_a\chi_{\text{Ni-Cu}}(T), \quad (7)$$

where  $N_a$  is the Avogadro number,  $\chi_{\text{Ni-Cu}}(T)$  is given by Eq. (6) and  $x'$  is the proportion of Cu-Ni pairs, which should be equal to the Ni concentration  $x$ . The constant  $\chi_0$  accounts for the various diamagnetic and paramagnetic contributions as explained in Eq. (1).  $\chi_{\text{pure}}(T)$  represents the susceptibility of the pure sample measured from 20 to 300 K and extrapolated below 20 K to  $1.35 \times 10^{-3}$  emu/mol at  $T=0$  (see Ref. 13). Very good fits of  $\chi(T)$  could be achieved by expression (7) from 20 to 300 K for all our Ni-doped samples ( $0.02 \leq x \leq 0.06$ ) and the obtained fitting parameters,  $\chi_0$ ,  $x'$  and  $\Delta$ , were found to be consistent for the various doping levels and field directions. Indeed, the  $\chi_0$  values remain very small ( $|\chi_0| < 0.09 \times 10^{-3}$  emu/mol in every fit), the  $x'$  values are equal to the  $x$  values within less than 15%, and the  $\Delta$  values are of the same order of magnitude for all concentrations and field directions. However, a slight difference is observed between the gap values obtained along the chain direction ( $c$ -axis) and perpendicular to the chain direction ( $a$  and  $b$ -axis), owing to the anisotropy which was not taken into account in this simple model: along  $c$ ,  $\Delta = (36 \pm 5)$  K, along  $a$  and  $b$ ,  $\Delta = (43 \pm 7)$  K, on the average for all the concentrations, leading to an exchange coupling  $J_{\text{Ni-Cu}} \approx 24-30$  K. Although the measured susceptibility cannot be well fitted by expression (7) below 20 K, one can notice that the fit has the correct shape: There is just a small shift in temperature. This shift is due to the interactions between the Cu-Ni pairs and with the rest of the Cu spins, which were not taken into account.

From the value of the energy gap, it is evident that the analysis of the susceptibility in  $\text{Cu}_{1-x}\text{Ni}_x\text{GeO}_3$ , performed

between  $T_N$  and  $T_{\text{SP}}$ , was altered by the existence of these AF Cu-Ni pairs, since this range of temperature corresponds to the crossover region between free  $S=1$  and  $S=1/2$  spins at high temperature and free  $1/2$  spins at low temperature. From the shape of the curve given by Eq. (7) in this crossover region, one can easily see that its effect on the previous analysis is an overestimation of the  $\chi_0$  constant and an underestimation of the proportion  $K_{\text{PARA}}$  of free  $1/2$  spins. One can then conclude that Ni-doping is effectively equivalent to Zn and Mg-doping and in particular that each Ni impurity is responsible, like Zn and Mg, for the freeing of one  $1/2$  spin at low temperature.

In summary, our susceptibility measurements for  $\text{Cu}_{1-x}M_x\text{GeO}_3$  (where  $M=\text{Zn, Mg, Ni}$ ) and for  $\text{CuGe}_{1-y}\text{Si}_y\text{O}_3$  establish a universal character with the scaling  $y \approx 3x$  for both the  $[T, x(y)]$  phase diagram and the mechanism of destruction of the SP phase, the latter being associated to the freeing of  $S=1/2$  Cu spins. The substitution of one Ge ion has the same effect as the substitution of three Cu ions and each substituted Cu ion leads to the freeing of one  $S=1/2$  Cu spin. Our results are consistent with the theoretical work of Khomskii *et al.*<sup>9</sup> However, Ni-doping shows some peculiarities, due to the magnetic and anisotropic nature of the Ni ion: The easy axis in the AF phase turns from the  $c$  to the  $a$ -axis and Ni-doping leads to the formation of AF Cu-Ni pairs. Experiments are in progress on other substitutions.

We would like to thank J. E. Lorenzo, P. Monod, and L.-P. Regnault for their interest in our work. We are also grateful to K. Katsumata and D. Khomskii for useful discussions.

\*Author to whom correspondence should be addressed at Institut d'Electronique Fondamentale, Bâtiment 220, Université Paris-Sud, 91405 Orsay Cedex, France. Electronic mail address: grenier@meige.ief.u-psud.fr FAX: 331 69 15 40 00.

<sup>1</sup>M. Hase, I. Terasaki, and K. Uchinokura, Phys. Rev. Lett. **70**, 3651 (1993).

<sup>2</sup>J.-P. Pouget, L.-P. Regnault, M. Ain, B. Hennion, J.-P. Renard, P. Veillet, G. Dhalenne, and A. Revcolevschi, Phys. Rev. Lett. **72**, 4037 (1994).

<sup>3</sup>J.-P. Renard, K. Le Dang, P. Veillet, G. Dhalenne, A. Revcolevschi, and L.-P. Regnault, Europhys. Lett. **30**, 475 (1995).

<sup>4</sup>M. Hase, I. Terasaki, Y. Sasago, K. Uchinokura, and H. Obara, Phys. Rev. Lett. **71**, 4059 (1993); S. B. Oseroff, S. W. Cheong, B. Aktas, M. F. Hundley, Z. Fisk, and L. W. Rupp, *ibid.* **74**, 1450 (1995); Y. Ajiro, T. Asano, F. Masui, M. Mekata, H. Aruga-Katori, T. Goto, and H. Kikuchi, Phys. Rev. B **51**, 9399 (1995); S. M. Coad, J. G. Lussier, D. F. McMorrow, and D. McK Paul, J. Phys.: Condens. Matter **8**, 6251 (1996).

<sup>5</sup>A. Revcolevschi and R. Collongues, C.R. Seances Acad. Sci.,

Ser. C **266**, 1767 (1969).

<sup>6</sup>G. Dhalenne, A. Revcolevschi, J.-C. Rouchaud, and M. Fedoroff, Mater. Res. Bull. **32**, 939 (1997).

<sup>7</sup>B. Grenier, J.-P. Renard, P. Veillet, C. Paulsen, R. Calemczuk, G. Dhalenne, and A. Revcolevschi, Phys. Rev. B **57**, 3444 (1998).

<sup>8</sup>Antiferromagnetic resonance experiments in  $\text{Cu}_{1-x}\text{Ni}_x\text{GeO}_3$  are also consistent with an easy axis along the  $a$  direction [K. Katsumata (private communication)].

<sup>9</sup>D. Khomskii, W. Geertsma, and M. Mostovoy, Czech. J. Phys. **46**, Suppl. S6, 3240 (1996).

<sup>10</sup>H. Fukuyama, T. Tanimoto, and M. Saito, J. Phys. Soc. Jpn. **65**, 1182 (1996).

<sup>11</sup>R. Kadano, J. Phys. Soc. Jpn. **66**, 505 (1997).

<sup>12</sup>K. M. Kojima, Y. Fudamoto, M. Larkin, G. M. Luke, J. Merrin, B. Nachumi, Y. J. Uemura, M. Hase, Y. Sasago, K. Uchinokura, Y. Ajiro, A. Revcolevschi, and J.-P. Renard, Phys. Rev. Lett. **79**, 503 (1997).

<sup>13</sup>G. Castilla, S. Chakraverty, and V. J. Emery, Phys. Rev. Lett. **75**, 1823 (1995).